IEEE Access
Multidisciplinary | Rapid Review | Open Access Journal

Received July 9, 2019, accepted July 30, 2019, date of publication August 2, 2019, date of current version August 19, 2019.

Digital Object Identifier 10.1109/ACCESS.2019.2932793

Interrupted-Sampling Repeater Jamming Suppression Based on Stacked Bidirectional Gated Recurrent Unit Network and Infinite Training

JIAN CHEN[1], SHIYOU XU[2], JIANGWEI ZOU[1], AND ZENGPING CHEN[2]

[1]National Key Laboratory of Science and Technology on ATR, College of Electronic Science and Technology, National University of Defense Technology, Changsha 410073, China

[2]School of Electronics and Communication Engineering, Sun Yat-sen University, Guangzhou 510275, China

Corresponding author: Shiyou Xu (xushy36@mail.sysu.edu.cn)

This work was supported in part by the Hunan Provincial Natural Science Foundation of China under Grant 2019JJ50715, and in part by the Scientific Research Projects of National University of Defense Technology under Grant ZK18-03-58.

ABSTRACT Interrupted-sampling repeater jamming (ISRJ) is coherent jamming based on digital radio frequency memory (DRFM) device, which repeatedly samples, stores, modulates, and retransmits part of the radar emitted signal, and flexibly forms false targets in the victim radar with relatively low transmitting power. It significantly interferes the radar to detect, track, and recognize targets. There are many electronic counter-countermeasures against ISRJ, among which a series of filtering methods are promising. However, it is not fully addressed. This study proposes a filtering method based on stacked bidirectional gated recurrent unit network (SBiGRU) and infinite training to fulfill the ISRJ suppression for pulse compression (PC) radar with linear frequency modulation (LFM) waveform. SBiGRU method converts signal extraction into a temporal classification problem and accurately extracts the jamming-free signal segments to generate a band pass filter to suppress the ISRJ and retain the real target signal components simultaneously. Comparing with two most advanced filtering methods in the published literature, SBiGRU method has improved the jamming-free signal extraction accuracy, leading to better performances of ISRJ suppression and real targets detection, which are verified by Monte Carlo Simulations.

INDEX TERMS Band pass filter, digital radio frequency memory (DRFM), electronic counter-countermeasure (ECCM), gated recurrent unit (GRU), infinite training, interrupted-sampling repeater jamming (ISRJ), signal extraction, temporal classification.

I. INTRODUCTION

Digital radio frequency memory (DRFM) [1] technique is widely applied in electronic countermeasure (ECM) field [2]–[5] since it has been proposed. Due to its ability to intercept, store and recall radio frequency signals, the signal retransmitted by a DRFM jammer is coherent with the emitted signal. Thus, a high processing gain can be obtained from signal processing such as pulse compression (PC) and coherent integration [6], [7]. Therefore, a DRFM jammer can flexibly form false targets in the victim radar with a relatively low transmitting power [8].

The associate editor coordinating the review of this manuscript and approving it for publication was Alma Y. Alanis.

DRFM jammers mainly work in two modes [9]–[13], i.e.: full-pulse-repeat-back mode and interrupted-sampling-repeating mode. When a DRFM jammer works in full-pulse-repeat-back mode, it intercepts, stores and retransmits the whole emitted signal pulse. While in interrupted-sampling repeating mode, the jammer samples a part of the pulse, retransmits it several times, and repeats the process until the pulse ends. This jamming is called interrupted-sampling repeater jamming (ISRJ), and a short name for this DRFM jammer in interrupted-sampling-repeating mode is ISRJer. ISRJers can be employed by unmanned aerial vehicles, planes, missiles, satellites, and so on, which significantly limits the ability of radar to detect, track and recognize those targets.

This work is licensed under a Creative Commons Attribution 4.0 License. For more information, see http://creativecommons.org/licenses/by/4.0/

Due to the flexibility of ISRJ, there are many jamming forms since it was proposed [12] in 2007, which can be roughly categorized into 2 classes: normal and modulation. In case of normal, the sampled signal segments are forwarded directly, whereas in case of modulation, they are modulated before retransmission. There is a special case of normal ISRJ proposed by Feng *et al.* [5] in 2014, which uses ISRJ to cancel linear frequency modulation (LFM) radar target echo, provided the range synchronization, phase coherent and amplitude matching requirements being met. It is an approach of active echo cancellation (AEC). The normal ISRJ forms a series of false targets which are farther than the real target in victim radar, which might exist some risks that the victim radar identifies the real target by range relationship. Li *et al.* [13] presented a modulation ISRJ method in 2014, which can form a train of false targets that precede the real one.

There are tremendous electronic counter-countermeasure (ECCM) techniques against ISRJ, which can be sorted into 2 main classes: active and passive methods.

In case of active methods, Hanbali and Kastantin [14] presented a technique to counter AEC based on ISRJ. It introduces a linear phase into the emitted signal, which not only eliminates the effect of the self-protective ISRJ, but also exploits the jamming signal power to augment the power of true target. Shen *et al.* [15] studied the performance of ISRJ based on intra-pulse frequency coded signal and found that the ISRJ of random frequency coded signal can only form a single false target in direct forwarding mode, which is different from a group of false targets of the ISRJ of LFM signal, and the ISRJ performance will be reduced with the increasing of the sub-pulse number. However, this kind of waveform cannot fully eliminate the false targets. Zhou *et al.* [7] presented an adaptive transmitting scheme for ISRJ suppression. The method firstly estimates the ISRJer working parameters such as slice width and beginning point of sampling by emitting normal waveform, then modifies the transmitted signal to make the ISRJ orthogonal to the reference signal. The performance of this method significantly depends on the accuracy of parameter estimation. And it will encounter failure if the ISRJ parameters are time varying.

The passive methods against ISRJ are mainly based on LFM waveform, and can be divided into 2 categories: ''reconstruction and cancellation'' approaches and filtering methods.

The idea of ''reconstruction and cancellation'' approaches were presented by Zhou C.'s group [16], [17]. This kind of approaches firstly estimate the ISRJ parameters such as the intercepted slice number and forwarding times by analyzing the PC results with time-frequency (TF) analysis, and estimate the slice width by deconvolution processing. Then, jamming signal is reconstructed according to the estimated parameters. Subsequently, the jamming is suppressed by iterative cancellation. However, the performance of ''reconstruction and cancellation'' approaches are sensitive to the parameter estimation precision, and the computational complexity is high due to the iterative processing.

The filtering methods to suppress ISRJ for LFM radar are promising, which extract the jamming-free signal segments in time domain, generate a band pass filter to suppress jamming in dechirped signal [18]–[21]. Gong *et al.* [18] proposed a filter generating method in 2014. The method calculates TF representation of the dechirped signal by short time Fourier transform (STFT), and an index function is obtained by summing the square of complex magnitude of TF representation in the frequency axis, which makes the index function vary with time. Then, it divides the radar receiving window into several segments and selects the time point with the minimum value of the index function in each segment, where the number of divisions is a hyper-parameter, and extracts dechirped signal segments with a preset length around these time points as jamming-free signal, where the segment length is another hyper-parameter. Subsequently, the band pass filter is generated from Fourier transform of the extracted signal for ISRJ suppression. Wei *et al.* [19] proposed an iterative approach in 2017 to exploit the method in [18] for wideband radar. The performance of this 2 methods depend severely on the two hyper-parameters. The optimal hyper-parameters are closely related with the ISRJer working parameters. Thus, the application of the method is significantly limited. H. Yuan, *et al.* proposed a filtering method based on the energy function of the dechirped signal [20] in 2017. The method calculates the minimum and maximum envelope of the energy function, and sets a threshold to the mean value of the minimum envelope. Then, it calculates the mean envelope of the maximum and minimum envelopes for jamming-free signal segments extraction. When the mean envelope is smaller than the threshold, the signal segment of the dechirped signal is extracted as jamming-free signal. There is no hyper-parameter for this method, making it applicable under all ISRJer working modes without adjusting the method. However, it suffers performance deterioration under low signal to noise ratio (SNR) and high jamming to signal ratio (JSR) conditions, due to the poor extraction accuracy of the jamming-free signal segments. Chen *et al.* [21] proposed a band pass filter design method based on the TF analysis, which is the state-of-the-art filtering method. The method automatically detects and extracts the jamming-free signal segments by a function constructed from the TF energy distribution of the de-chirped signal, named max-TF function. A two-stage thresholds strategy is employed in the extraction. The filter generated from the jamming-free signal segments is smoothed to make the filtered PC results being suitable for constant false alarm rate (CFAR) detectors. The method has improved the extraction accuracy, leading to a higher suppression performance and extended feasible scope of SNR and JSR than the previous filtering methods. However, the extraction accuracy could be further improved, since the noise segment elimination approach used in [21] is imprecise and may be misled by frequency shifted ISRJ.

Inspired by the powerful classification and regression ability of deep learning networks [22]–[25], especially the temporal classification of recurrent neural networks, such as long

short term memory (LSTM) network [26]–[28] and gated recurrent unit (GRU) [28], [29], this paper proposes a more powerful jamming-free signal segments extraction method to generate a more powerful filter for ISRJ suppression. The main contributions of this work can be concluded as follows:

1) This work converts the jamming-free segments extraction into a temporal classification problem, and a stacked bidirectional gated recurrent unit (SBiGRU) network is designed to perform the classification. SBiGRU method extracts jamming-free signal more accurately and has higher performances of jamming suppression and real target detection than the method in the published literature.
2) This work introduces a concept of ''infinite training''. The SBiGRU network is trained by infinite samples generated according to the signal model until the loss function decreases no more. Since the training dataset is infinite and can fully represent the problem, there is no risk of overfitting, which is usually a big trouble for finite training.

The remaining contents of this paper are organized as follows: In section II, the signal model of LFM radar and ISRJ working principle are introduced. In section III, the proposed method is detailed, including the framework, preprocessing, SBiGRU network design, and training. Section IV describes the simulations for comparing the performance of the proposed method and 2 most advanced filtering methods in the published literature. In section V, the results and analysis are presented. Conclusions are drawn in section VI.

II. SIGNAL MODEL

The dechirping radar transmits LFM signal pulse and receives pulse echoed by targets. The received pulse is dechirped, which converts every signal component echoed by a single target to a single-frequency signal. Then the PC result is obtained from the dechirped signal by Fourier transform, displaying the target in relative range (frequency) domain. If there is a target carrying an ISRJer in radar sight, the received pulse will be contaminated by ISRJ signal components, and ISRJ components will be converted to several single-frequency components.

The normalized LFM signal pulse $s(t)$ emitted by radar is expressed as follows [30], [31]:

$$s(t) = \text{rect}\left(t/T_p\right)\exp\left(j\pi Kt^2\right) \tag{1}$$

where

$$\text{rect}\left(\frac{t}{T_p}\right) = \begin{cases} 1, & 0 \le t \le T_p \\ 0, & \text{otherwise} \end{cases} \tag{2}$$

is a rectangular window function with pulse width T_p and initial location 0; K is the frequency modulation rate. The carrier frequency of the signal is neglected since it has no effect on the deductions in this paper.

Signal echoed by a target to the radar is formulated below:

$$s_{\text{tar}}(t) = A_{\text{tar}}\, s(t - \tau_{\text{tar}}) \tag{3}$$

where A_{tar} is a constant, representing the amplitude of the target signal; τ_{tar} is the time delay and $\tau_{\text{tar}} = 2R_{\text{tar}}/c$, where c denotes the speed of light and R_{tar} is the distance between the target and radar, also called the range of target.

The ISRJer samples a slice of the radar emitted signal, then retransmits the slice several times. The sampling-retransmitting process is repeated until the radar signal pulse ends, as shown in Fig. 1.

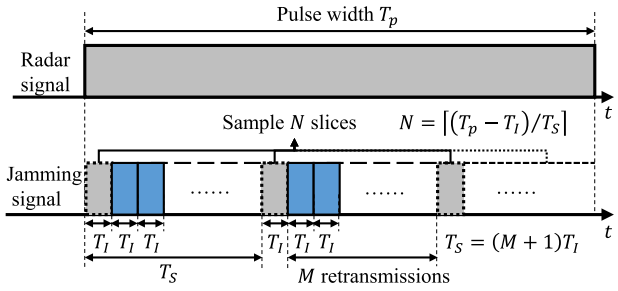

FIGURE 1. The principle of ISRJ.

The interrupted sampling function is defined as follows [12], [17]:

$$p(t) = \sum_{n=1}^{N} \text{rect}\left(\frac{t - nT_S}{T_I}\right) \tag{4}$$

where T_I is the slice width; $T_S = (M+1)T_I$, representing the time interval between adjacent intercepted slices, of which M stands for the number of retransmissions of each slice; and $N = \lceil (T_p - T_I)/T_S \rceil$, denoting the number of slices that can be sampled during a pulse.

Therefore, the sampled signal $s_I(t)$ can be expressed as follows:

$$s_I(t) = p(t - \tau_{\text{tar}})\, s(t - \tau_{\text{tar}}). \tag{5}$$

After sampling, every sampled slice is retransmitted M times. Thus, the jamming signal $s_J(t)$ received by radar is formulated as follows:

$$s_J(t) = A_J \sum_{m=1}^{M} s_I(t - mT_I) \tag{6}$$

where A_J is the amplitude of the jamming signal.

Therefore, the radar received signal can be expressed as:

$$s_r(t) = s_{\text{tar}}(t) + s_J(t) + n(t) \tag{7}$$

where $n(t)$ is white Gaussian noise.

The reference signal $s_{\text{ref}}(t)$ is a time delayed version of the transmitted signal but not rectangular windowed, i.e.:

$$s_{\text{ref}}(t) = \exp\left[j\pi K(t - \tau_{\text{ref}})^2\right] \tag{8}$$

where the time delay $\tau_{\text{ref}} = 2R_{\text{ref}}/c$, corresponding to a reference range R_{ref}, which is preset by the radar system.

The dechirped signal $s_d(t)$ is obtained by multiplying the received signal $s_r(t)$ and the reference signal $s_{\text{ref}}(t)$:

$$\begin{aligned} s_d(t) &= s_r^*(t) s_{\text{ref}}(t) \\ &= \left[s_{\text{tar}}(t) + s_J(t) + n^*(t)\right] s_{\text{ref}}(t) \\ &= s_{d,tar}(t) + s_{d,J}(t) + v(t) \end{aligned} \tag{9}$$

where

$$s_{d,\mathrm{tar}}(t) = A_{\mathrm{tar}}\,\mathrm{rect}\left[(t-\tau_{\mathrm{tar}})/T_p\right] \times e^{j\pi K\left[2(\tau_{\mathrm{tar}}-\tau_{\mathrm{ref}})t+\tau_{\mathrm{ref}}{}^2-\tau_{\mathrm{tar}}{}^2\right]}, \quad (10)$$

and

$$s_{d,J}(t) = A_J \sum_{m=1}^{M}\sum_{n=1}^{N}\mathrm{rect}\left[\frac{t-\tau_{\mathrm{tar}}-mT_I-nT_S}{T_I}\right] \times e^{j\pi K\left[2(\tau_{\mathrm{tar}}+mT_I-\tau_{\mathrm{ref}})t+\tau_{\mathrm{ref}}{}^2-(\tau_{\mathrm{tar}}+mT_I)^2\right]}. \quad (11)$$

Equations (9)-(11) indicate that the dechirped signal is composed of single-frequency components and noise, which means that the jamming components could be suppressed by a well-designed filter.

III. METHOD

The basic idea of filtering methods against ISRJ is extracting jamming-free segments of the dechirped signal in time domain to generate a band pass filter to suppress the ISRJ signal components. The jamming-free segments are not contaminated by the jamming, therefore, the spectrum of jamming-free signal only contains the frequency components of real targets, which is very suitable to be used as a band pass filter to suppress the ISRJ. The basic process flowchart of filtering methods is shown in Fig. 2.

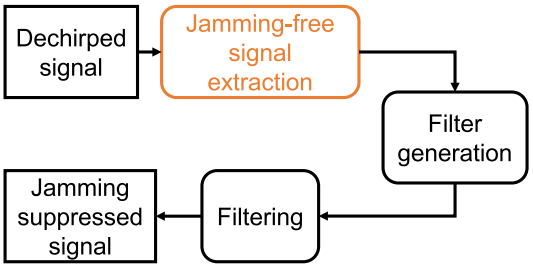

FIGURE 2. The basic flowchart of filtering methods.

The proposed SBiGRU method follows the basic flowchart in Fig. 2, but it thoroughly innovates the jamming-free signal extraction, that the signal extraction problem is converted into a temporal classification task. The flowchart of SBiGRU method's jamming-free signal extraction is depicted in Fig. 3.

As Fig. 3 illustrated, the jamming-free signal extraction of SBiGRU method consists of 3 main steps:

1) Preprocessing. The dechirped signal is pre-processed to form the input of SBiGRU network.
2) Classification. SBiGRU network outputs the signal component class ID, which is a time-varying sequence, with the same length of the dechirped signal.
3) Extraction. The jamming-free signal is obtained by extracting segments of dechirped signal when the signal component class ID indicates the signal is jamming-free.

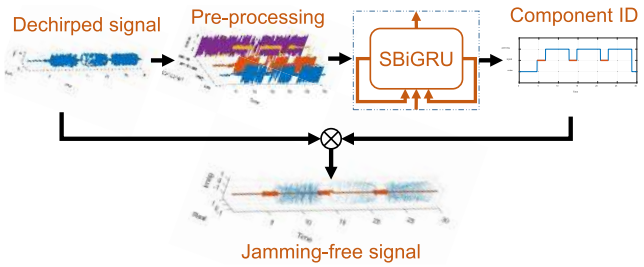

FIGURE 3. The jamming-free signal extraction flowchart of SBiGRU method.

After extraction, the jamming-free signal is utilized to generate a band pass filter, i.e.:

$$H(f) = \frac{\mathcal{F}\{s_c(t)\}}{\max\left(|\mathcal{F}\{s_c(t)\}|\right)} \quad (12)$$

where $s_c(t)$ is the jamming-free signal extracted by SBiGRU method, $\mathcal{F}\{\cdot\}$ stands for Fourier transform.

Then $H(f)$ is smoothed to make noise background of the final PC result suitable for constant false alarm rate (CFAR) target detection [21]. $H(f)$ is squared, and then detected by a CFAR detector with a relatively high false alarm probability. At each cell where a "target" is detected, the smoothed filter $H_s(f)$ holds the value of $H(f)$, while in each interval between two adjacently detected cells, the value of $H_s(f)$ is set to the average value of $H(f)$ in the interval.

The final PC result $r(f)$ is obtained by the formula as below:

$$r(f) = \mathcal{F}\{s_d(t)\}\,|H_s(f)|\,. \quad (13)$$

A. PREPROCESSING

The preprocessing involves two steps: amplitude normalization and temporal real value sequences generation.

The amplitude normalization can be expressed by the formula below:

$$x_a(n) = \frac{x_d(n)}{\max\limits_n |x_d(n)|}, \quad n = 1, 2, \ldots, N \quad (14)$$

where $x_d(n)$ denotes the discrete time representation of the dechirped radar pulse signal $s_d(t)$, and N is the number of sampling points of a signal pulse.

The amplitude normalization reduces the complexity of inputs by one degree of freedom, which helps the SBiGRU network focus on the signal fluctuations to do classification.

Based on the normalized sequence of dechirped signal $x_a(n)$, 4 temporal real value sequences are generated, i.e.:

$$\begin{aligned} x_1(n) &= \mathrm{real}[x_a(n)] \\ x_2(n) &= \mathrm{imag}[x_a(n)] \\ x_3(n) &= |x_a(n)| \\ x_4(n) &= \mathrm{angle}[x_a(n)] \end{aligned} \quad (15)$$

where $x_1(n)$ is the real part sequence of $x_a(n)$, $x_2(n)$ the image part sequence, $x_3(n)$ the amplitude sequence, and $x_4(n)$ the angle sequence.

The 4 sequences are compounded side by side to form the input $x(n)$ of SBiGRU network, namely, an $N \times 4$ tensor, which indicates that, at any temporal step n, a 4-element vector, i.e. $x(n) = [x_1(n), x_2(n), x_3(n), x_4(n)]$, is input into the SBiGRU network.

B. SBIGRU NETWORK

The SBiGRU network consists of 4 stacked bidirectional gated recurrent unit (GRU) layers and 2 dense layers, of which the structure is descried in Table 1, where "Params. Num." stands for "number of trainable parameters".

TABLE 1. Structure of SBiGRU network.

Layer	Output Shape	Params. Num.*
Input Placeholder	[N, 4]	0
Bidirectional GRU 1	[N, 40*2]	11040
Bidirectional GRU 2	[N, 30*2]	20160
Bidirectional GRU 3	[N, 20*2]	9840
Bidirectional GRU 4	[N, 15*2]	5130
Dense 1 [a]	[N, 16]	496
Dense 2 [b]	[N, 3]	51

[a] The activation for layer "Dense 1" is ReLU [32].
[b] The activation for layer "Dense 2" is Softmax [33].
* The total number of trainable parameters is 46717.

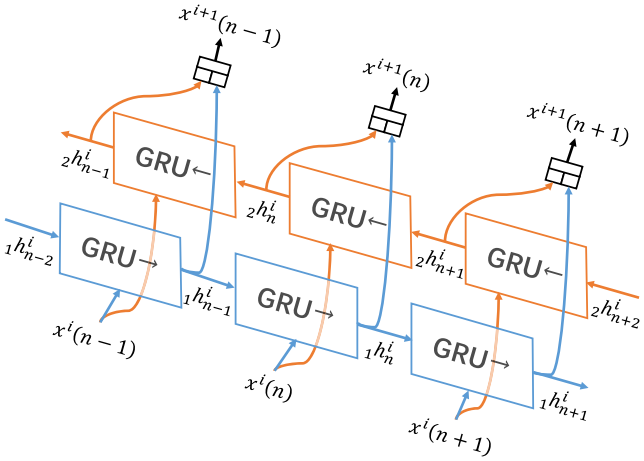

FIGURE 4. Data flow of bidirectional GRU layer.

The data flow of the ith bidirectional GRU layer is illustrated in Fig.4. There are two standard GRUs working along two opposite temporal directions in each bidirectional GRU layer, as shown in Fig.4. $x^i(n)$ is the input vector of the ith bidirectional GRU layer at the temporal step n, and $x^{i+1}(n)$ is the output vector, obtained by concatenating the hidden state vectors of the two GRUs, i.e.: ${}_1h_n^i$ and ${}_2h_n^i$. The output vectors of the ith layer are the input vectors of the $(i+1)$th layer.

According to Table 1, there are 40, 30, 20, and 15 elements of ${}_1h_n^i$ and ${}_2h_n^i$, for $i = 1$, 2, 3, and 4, respectively. "Dense 1" takes a 30-elements vector as input, and outputs a 16-elements vector at each temporal step. Its activation function is ReLU. "Dense 2" is the output layer with a Softmax activation. It output a 3-elements vector for each temporal step, implying the probability of the signal at this temporal step is noise, jamming-free signal or contaminated by ISRJ. In training phase, the 3-elements vector is used to calculate the loss, which is detailed in Section III-C. In prediction phase, it is utilized to do the classification, i.e.: the index of the maximum element of the vector is the class ID of the signal at current temporal step.

C. INFINITE TRAINING

Radar received pulses which are contaminated by ISRJ can be generated according to Section II. For training samples generation, the parameters' setting rules are listed in Table 2.

TABLE 2. Infinite training samples generating parameters' setting rules.

Parameter	Setting Rule
Sampling frequency(f_s)	Normalized to unit 1
Receiving gate width (T_g) [a]	$500 \le T_g \le 2500, T_g \in \mathbb{N}$
Radar pulse width (T_p) [b]	$[0.7, 1.2] \cdot T_g$
Pulse bandwidth (B)	$[0.5, 0.95]$
Frequency modulation rate (K)	$\pm B/T_p$
Lowest frequency (f_0) of a pulse	$[0.15, 0.95] \cdot (1 - B)$
Echo pulse initial time (t_d) relative to up edge of receiving gate	$\begin{cases} [T_p - T_g, T_g - T_p] & \text{if } T_p \le T_g \\ [T_g - T_p, 0] & \text{if } T_p > T_g \end{cases}$
Slice width (T_I) of ISRJer	$[20, \frac{1}{3}T_g]$
ISRJer working mode (M_o)	{0,1,2,3,4,5} [c]
SNR (SNR)	$[-20, 20]$ dB
JSR (JSR)	$[0, 50]$ dB

[a] The unit for (T_g) is point, in accord with the sampling frequency.
[b] The range of T_p means that the pulse width might be larger than the receiving gate. This is designed only for training, to simulate the situations that partial real target echo are not included in the receiving gate.
[c] If $M_o = 0$, ISRJer intercepts only one slice and retransmits it over and over until the radar pulse ends; otherwise, ISRJer retransmits the intercepted slices M_o times.

The parameters for radar emitter, receiver, target, ISRJer, and noise environment are randomly generated according to Table 2. If a parameter is set to an interval or several cases, it obeys uniform distribution.

Since the sampling frequency is normalized to unit 1, most situations of ISRJ contaminated echo signal pulses of narrowband radar can be included in the settings.

The designed loss function to be minimized is a weighted categorical cross entropy, i.e.:

$$J = -\sum_{i=1}^{Nc}\sum_{j=1}^{N} w_i y_{i,j}^{\text{true}} \ln(y_{i,j}^{\text{pred}}) \tag{16}$$

where Nc is the number of signal component classes; w_i is the weight for the ith class; $y_{i,j}^{\text{true}}$ is the indicator of the ith class at the jth temporal step; and $y_{i,j}^{\text{pred}}$ is the output value of SBiGRU network for the ith class at the jth temporal step, implying the probability of the signal at the jth temporal step belongs to the ith class in the training phase. $Nc = 3$, and the class IDs $\{1, 2, 3\}$ indicate that the signal at a certain moment is noise, real target echo plus noise (target), and signal contaminated by jamming (jamming), respectively. $w = [1, 1, 2]$. The weight for the 3rd class is doubled, for not mis-classifying the jamming to be other classes. If the signal at the jth temporal

step belong to the ith class, $y_{i,j}^{\text{true}} = 1$; otherwise, $y_{i,j}^{\text{true}} = 0$. $\sum_{i=1}^{Nc} y_{i,j}^{\text{pred}} = 1$.

Adadelta [34] optimizer is utilized in SBiGRU method. It's a more robust extension of Adagrad [35] that adapts learning rates based on a moving window of gradient updates, instead of accumulating all past gradients.

A training epoch has 10 batches. A batch contains 200 samples of generated signal pulses. The receiving gate width is invariant during 50 epochs in training phase, but it is regenerated in the next 50 epochs.

The network is trained on the infinitely generated samples until the loss function decreases no more.

IV. SIMULATIONS

In order to show the performance advantages of the proposed method over other filtering methods in the published literature and to demonstrated how SNR and JSR conditions affact the performance, a series of Monte Carlo simulations were designed.

The proposed SBiGRU method was compared with the 2 most advanced filtering methods, which were referred to as *energy* [20] and *max-TF* [21] methods in this paper. Our method and the 2 competitors were tested under different ISRJer parameters, SNR, and JSR conditions.

The parameters of radar and target for generating test-samples are listed in Table 3.

TABLE 3. Parameters of radar and target for testing samples.

Parameter	Value
Complex sampling frequency(f_s)	50 MHz
Receiving gate width (T_g)	30 μs
Radar pulse width (T_p)	20 μs
Pulse bandwidth (B)	40 MHz
Frequency modulation rate (K)	B/T_p
Carrier frequency (f_0)	6 GHz
Target relative range (f_0)	679.5 m

TABLE 4. ISRJer parameters of 5 working mode.

Mode No.	Retransmition Times (M)	Number of Slices (N)	Jam.-free Duty Ratio
1	9	1	10%
2	4	2	20%
3	3	3	30%
4	2	4	40%
5	1	5	50%

The target holds an ISRJer with slice width $T_I = 2\mu$s. The ISRJer has 5 working modes, of which the parameters are listed in Table 4, where ''Jam.-free Duty Ratio'' means the ratio of the jamming-free signal time duration to the radar pulse width. ISRJer shifted the frequency of the sampled signal by 6 MHz.

In order to show how SNR and JSR affect the filtering performance, SNR ranged from -20 to 20 dB with an interval of 2.5dB, and JSR ranged from 5 to 50 dB with an interval of 5 dB.

The 5 ISRJ modes, 17 SNR and 10 JSR conditions, made 850 condition combinations. The 3 methods were applied to all the 850 conditions, each for a 1500 repetitions' Monte Carlo simulation. Additionally, no-jamming case under the 17 SNR conditions were put through the same Monte Carlo simulation.

The jamming-free signal extraction results, the amplitudes of real target and the maximum ones at other locations in PC results which are not filtered and filtered by the 3 methods, and the target detection results were recorded. First order difference CFAR (FOD-CFAR) [36] detector was employed for target detection due to its effectiveness and robustness. The false alarm rate of FOD-CFAR detector was set to 10^{-5}.

V. RESULTS AND ANALYSIS

A. EXTRACTION ACCURACY

The best situation of the extraction is that all the jamming-free segments are extracted and no other signal segments are mistakenly extracted.

Recall rate was employed to measure how much of the jamming-free signal was extracted from the total jamming-free signal. The definition is expressed as follows:

$$P_{\text{recall}} = \frac{N_{\text{JFE}}}{N_{\text{JF}}} \tag{17}$$

where N_{JFE} stands for the point numbers of correctly extracted jamming-free segments, and N_{JF} is that of the total jamming-free segments under certain conditions.

Since there were two kinds of other signal segments, i.e., noise segments and jamming-contaminated segments, **noise rate** and **jamming rate** were utilized to measure how much of the extracted jamming-free signal was mis-extracted from noise and jamming-contaminated segments, respectively. The calculation formulas are expressed below:

$$P_{\text{noise}} = \frac{N_{\text{NE}}}{N_{\text{E}}} \tag{18}$$

$$P_{\text{jamming}} = \frac{N_{\text{JE}}}{N_{\text{E}}} \tag{19}$$

where N_{NE} and N_{JE} are the points number of the noise and jamming-contaminated segments which are extracted as jamming-free signal, and N_{E} is the total points number of the extracted segments under certain conditions.

For recall rate, the larger value indicates higher performance of the generated filter under all SNR and JSR conditions. In the contrary, for noise rate or jamming rate, the smaller value is better. To be more specific, lower noise rate is more useful under low SNR conditions, and lower jamming rate plays a more important role under high JSR conditions.

The 3 metrics of the 3 methods vs SNR and JSR are depict in Fig. 5, where ''jam. rate'' is short for jamming rate. The value in each SNR-JSR grid is averaged under 5 ISRJer's working mode, each with 1500 repetitions, and the unit is one thousandth. The 3 panels (a,b,c) in the 1st row are results of recall rate; those in the 2nd row are results of noise rate; and those in the 3rd row are results of jamming rate.

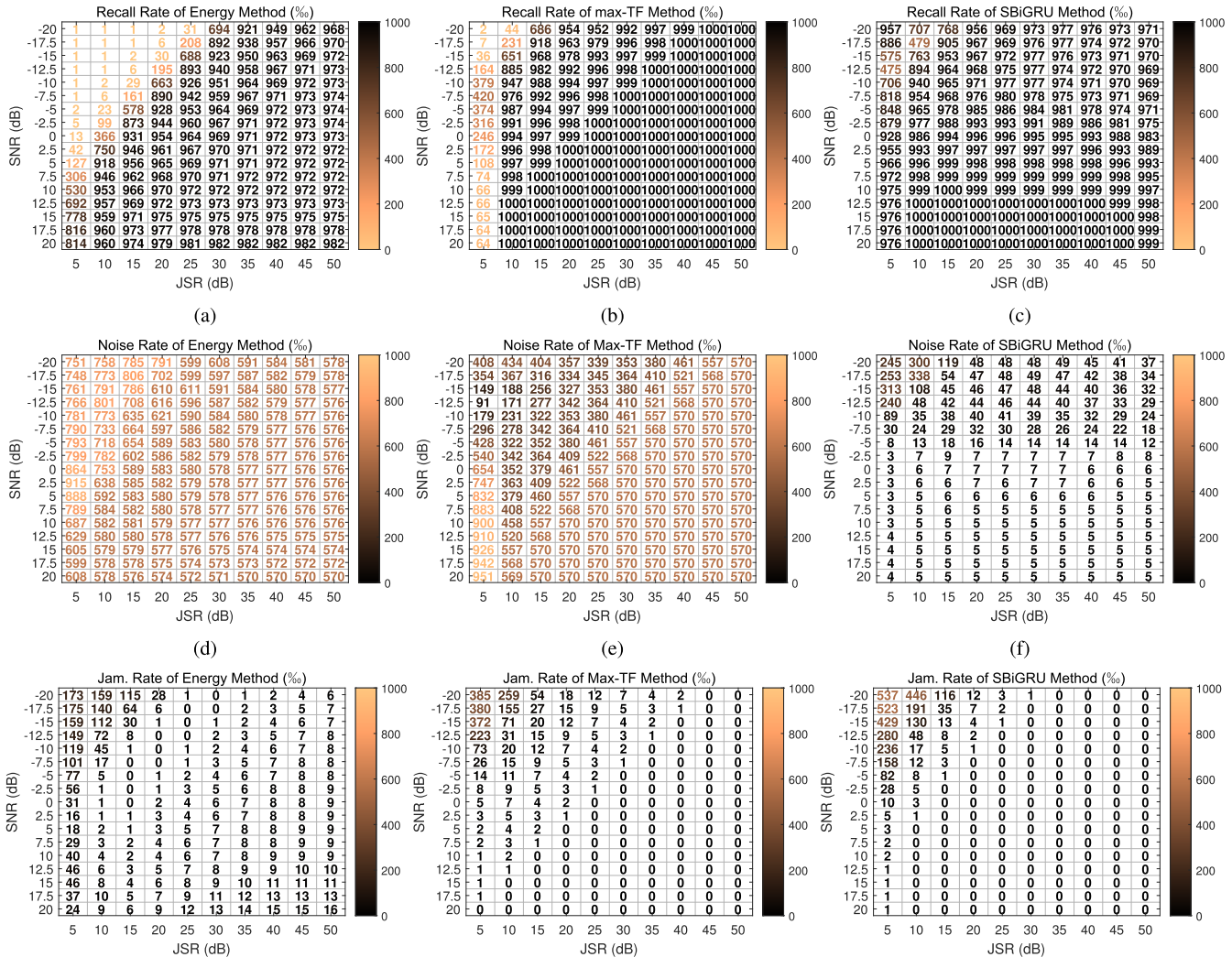

FIGURE 5. The recall rate, noise rate, and jamming rate vs SNR & JSR of *energy*, *max-TF*, and SBiGRU methods.

From Fig. 5, we could see some facts:

1) Considering recall rate, *energy* and *max-TF* methods performed relatively well under high SNR or high JSR conditions, whereas relatively bad under low SNR and low JSR conditions, and the proposed SBiGRU method performed relatively well under nearly all the tested SNR and JSR conditions. In general, SBiGRU method significantly outperformed the 2 competitors under low SNR and low JSR conditions, and is superior to or comparable with them under other SNR and JSR conditions.
2) Considering noise rate, SBiGRU method was significantly better than the 2 competitors under all the tested SNR and JSR conditions, and *max-TF* method performed better than *energy method*.
3) Considering jamming rate, SBiGRU method performed better than the 2 competitors under relatively high JSR or high SNR conditions, and it was not as good as them under low JSR and low SNR conditions.

From the facts, it seems that SBiGRU method "knows" how to behavior under a certain condition to achieve the best performance, as it has a lower noise rate under low SNR conditions and lower jamming rate under high JSR conditions comparing with *max-TF* and *energy* methods. We could infer that SBiGRU method will have a better jamming suppression and detection performance than the 2 competitors.

B. JAMMING SUPPRESSION AND REAL TARGET RETAINING PERFORMANCE

The jamming suppression and real target retaining ability of the 3 methods are measured by the metric of "signal to jamming ratio improvement factor (**SJRIF**)" [21]. Before defining SJRIF, signal to jamming ratio (SJR) in a PC result

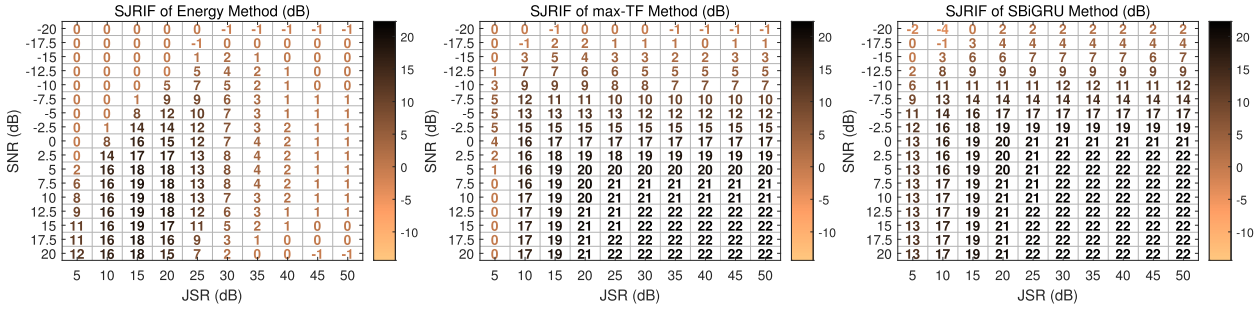

FIGURE 6. The SJRIF vs SNR & JSR of (a) *energy*, (b) *max-TF*, and (c) SBiGRU methods.

$r(f)$ is defined as follows:

$$\mathrm{SJR} = 20\log_{10}\left(a_t/a_j\right) \tag{20}$$

where $a_t = |r(f_{\mathrm{tar}})|$ stands for the amplitude of real target with f_{tar} indicating the range of real target, and $a_j = \max_{f\neq f_{\mathrm{tar}}}(|r(f)|)$ is the maximum amplitude of jamming or noise. Then, SJRIF can be expressed as:

$$\mathrm{SJRIF} = \mathrm{SJR}_{\mathrm{filtered}} - \mathrm{SJR}_{\mathrm{unfiltered}} \tag{21}$$

where $\mathrm{SJR}_{\mathrm{filtered}}$ is SJR of a filtered PC result, and $\mathrm{SJR}_{\mathrm{unfiltered}}$ is that of the raw PC result that not filtered.

The SJRIF results vs SNR & JSR of the 3 methods are depicted in Fig. 6.

As shown in Fig. 6, we could see that:

1) SBiGRU method had higher or equivalent SJRIF comparing with *energy* and *max-TF* methods under all tested SNR and JSR conditions except for 2 SNR-JSR girds (SNR:-20; JSR:5,10).
2) *Max-TF* method outperformed *energy* method under most SNR-JSR grids.
3) For SBiGRU and *max-TF* methods, SJRIF get higher as the SNR or JSR increases. This is a result of that the extraction becomes more accurate as SNR or JSR increases.
4) The SJRIF of *energy* method stays relatively high in a limited SNR-JSR region (approximately, 2.5dB $\leq$ SNR $\leq$ 17.5dB, 10dB $\leq$ JSR $\leq$ 25dB). It is a result from the recall rate, noise rate, and jamming rate.

C. DETECTION PERFORMANCE

The detection performance of radar after employing filters is demonstrated by **detection rate**, which is defined as follows:

$$P_d = N_d/N_{\mathrm{total}}. \tag{22}$$

where N_d is the number of detected targets, and N_{total} is the total number of targets which exist in the PC results.

The detection results of FOD-CFAR detector employed on the PC results which are not filtered and filtered by the 3 methods are plotted in Fig. 7. There are 11 cures in every panel of Fig. 7. One of the 11 cures is the detection rate cures under no jamming conditions, and the other 10 are under different JSR conditions from 5 dB to 50 dB.

Comparing the detection results of the 4 cases, we could see that:

1) The detection rate cures of the 4 cases are nearly the same under no jamming conditions, implying that the 3 filtering methods do not affect radar detection performance under such conditions.
2) By applying any one of the 3 methods, detection rate improved under most SNR and JSR conditions, except for no jamming situations.
3) The detection performance of PC results filtered by SBiGRU method is the highest among the 4 cases. It is a natural result of the best jamming-free signal extraction and the highest SJRIF.
4) The detection rates of the 4 cases decrease as JSR increases.

In general, the detection rate increases as the SNR increases. However, in Fig. 7 (b), the detection rate firstly increases as the SNR increases and then decreases as the SNR increases further, when 30 $\leq$ JSR $\leq$ 40 dB. The reason is that, in low SNR region, the recall rate of *energy* method increases as SNR becomes larger, leading to the increase of SJRIF and detection rate, and in high SNR region, the jamming rate increases as SNR increases whereas the recall rate and noise rate are stable, resulting in the deterioration of the SJRIF and detection rate.

The detection rate of SBiGRU and *max-TF* method with low JSR under low SNR conditions is higher than that of no jamming case. The reason is that the real targets are enhanced by the filters generated by the 2 method under such conditions when the JSR is low whereas the filters of no jamming case are all-pass filter

D. TIME CONSUMPTION

Since the jamming suppression algorithms are intended to real-time applications, we recorded the time consumption of the 3 methods for radar system designers. In order to measure the time consumption, we applied the 3 methods to 1000 testing pulses on a workstation with an i9-9900K CPU and a GTX 1080Ti GPU. All the processes of *Energy* and *max-TF* methods were executed by single thread Matlab codes on CPU. The processes of SBiGRU method were executed by the same means except that the jamming-free

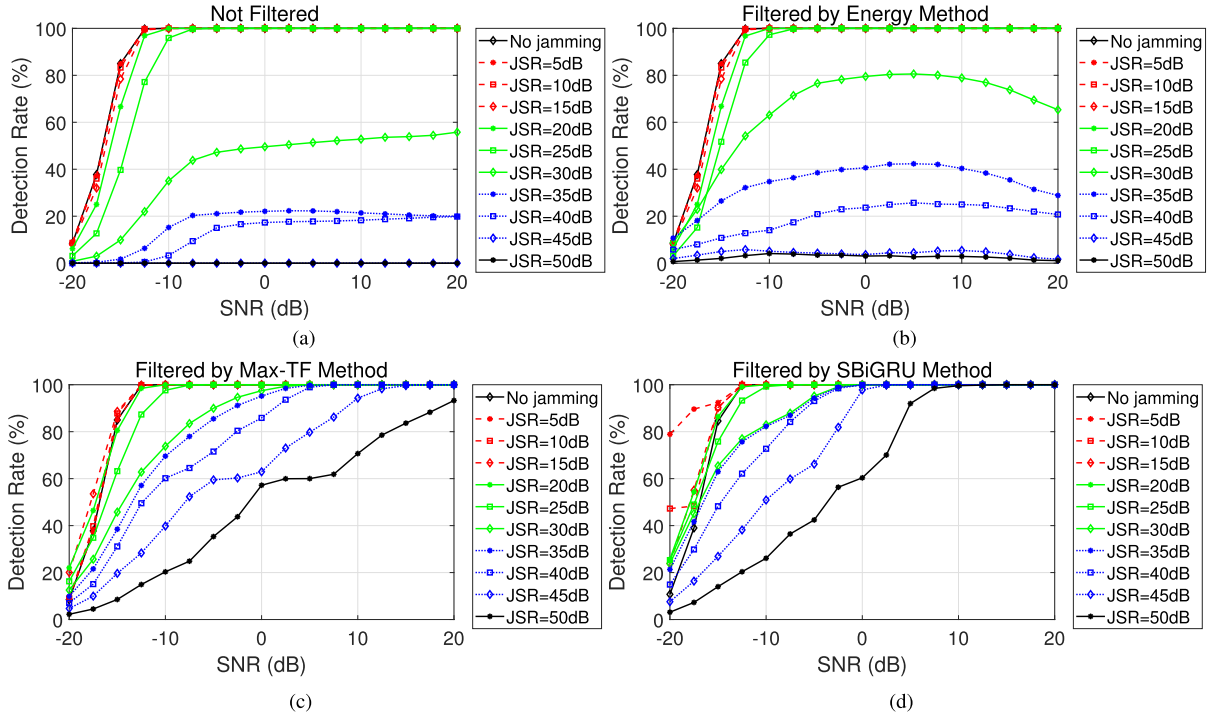

FIGURE 7. The detection rate cures. (a) Not filtered, (b) filtered by *energy* method, (c) filtered by *max-TF* method, (d) filtered by SBiGRU method.

signal extraction of SBiGRU method was executed by Keras codes on GPU, which significantly accelerates the computing speed of SBiGRU network. The time consumption results are described in Table 5.

TABLE 5. Time consumption for filtering 1000 testing pulses.

Method	Extraction (s)	Filter Generation and Filtering (s)	Total Time Consumption (s)
Energy	1.40	12.74	14.14
Max-TF	22.71	12.77	35.48
SBiGRU	0.64 *	12.76	13.40

* The jamming-free signal extraction of SBiGRU method was accelerated by GPU.

The results in Table 5 demonstrate that: the time consumption of "filter generation and filtering" are nearly the same for the 3 methods, since those processes are exactly the same; the time consumption of "extraction" for *max-TF* method is about 15 times of that for *energy* method, and that for SBiGRU method is the shortest with help of a powerful GPU.

Theoretically, the comparison of computational complexity of jamming-free signal extraction for the 3 methods is: *energy* < *max-TF* < SBiGRU, and the computational complexity of extraction for SBiGRU is approximately 5 times of that for *max-TF* method. However, with the help of GPU, the time consumption of SBiGRU is significantly reduced, indicating that it potentially be capable for real-time applications.

VI. CONCLUSION

We constructed a temporal classifier based on SBiGRU and infinitely trained it for extracting jamming-free signal from ISRJ contaminated radar received signal, achieving intelligently better extraction accuracy under different SNR and JSR conditions, leading to more powerful ISRJ suppression ability and higher real target detection performance when compared with the 2 most advanced filtering methods against ISRJ. The proposed method paves a way for radar to detect and further to track and recognize real targets in ISRJ environment.

In the near future, we will work on improving the radar detection and tracking performance through multi-pulses processing in ISRJ environment, on the foundation of single pulse detection which is addressed by the proposed method in this paper.

REFERENCES

[1] S. J. Roome, "Digital radio frequency memory," *Electron. Commun. Eng. J.*, vol. 2, no. 4, pp. 147–153, Aug. 1990. doi: 10.1049/ecej:19900035.
[2] P. C. J. Hill and V. Truffert, "Statistical processing techniques for detecting DRFM repeat-jam radar signals," in *Proc. IEE Colloq. Signal Process. Techn. Electron. Warfare*, Jan. 1992, pp. 1–6.
[3] S. D. Berger, "Digital radio frequency memory linear range gate stealer spectrum," *IEEE Trans. Aerosp. Electron. Syst.*, vol. 39, no. 2, pp. 725–735, Apr. 2003. doi: 10.1109/taes.2003.1207279.
[4] D. Feng, H. Tao, Y. Yang, and Z. Liu, "Jamming de-chirping radar using interrupted-sampling repeater," *Sci. China, Ser. F, Inf. Sci*, vol. 54, no. 10, pp. 2138–2146, Oct. 2011. doi: 10.1007/s11432-011-4431-4.
[5] D. Feng, L. Xu, W. Wang, and H. Yang, "Radar target echo cancellation using interrupted-sampling repeater," *IEICE Electron. Exp.*, vol. 11, no. 8, pp. 1–6, Apr. 2014. doi: 10.1587/elex.11.20130997.
[6] K. Olivier, J. E. Cilliers, and M. du Plessis, "Design and performance of wideband DRFM for radar test and evaluation," *Electron. Lett.*, vol. 47, no. 14, pp. 824–825, 2011. doi: 10.1049/el.2011.0362.
[7] C. Zhou, F. Liu, and Q. Liu, "An adaptive transmitting scheme for interrupted sampling repeater jamming suppression," *Sensors*, vol. 17, no. 11, p. 2480, 2017. doi: 10.3390/s17112480.

[8] Z. Wei, Z. Liu, B. Peng, and R. Shen, "ECCM scheme against interrupted sampling repeater jammer based on parameter-adjusted waveform design," *Sensors*, vol. 18, no. 4, p. 1141, 2018.
[9] M. Greco, F. Gini, and A. Farina, "Radar detection and classification of jamming signals belonging to a cone class," *IEEE Trans. Signal Process.*, vol. 56, no. 5, pp. 1984–1993, May 2008.
[10] J. Zhang, D. Zhu, and G. Zhang, "New antivelocity deception jamming technique using pulses with adaptive initial phases," *IEEE Trans. Aerosp. Electron. Syst.*, vol. 49, no. 2, pp. 1290–1300, Apr. 2013.
[11] Y. Lu and S. Li, "CFAR detection of DRFM deception jamming based on singular spectrum analysis," in *Proc. IEEE Int. Conf. Signal Process., Commun. Comput.*, Xiamen, China, Oct. 2017, pp. 1–6.
[12] W. XueSong, L. JianCheng, Z. WenMing, F. QiXiang, L. Zhong, and X. XiaoXia, "Mathematic principles of interrupted-sampling repeater jamming (ISRJ)," *Sci. China F, Inf. Sci.*, vol. 50, no. 1, pp. 113–123, Feb. 2007. doi: 10.1007/s11432-007-2017-y.
[13] C.-Z. Li, W.-M. Su, H. Gu, C. Ma, and J.-L. Chen, "Improved interrupted sampling repeater jamming based on DRFM," in *Proc. IEEE Int. Conf. Signal Process., Commun. Comput.*, Guilin, China, Aug. 2014, pp. 254–257.
[14] S. B. S. Hanbali and R. Kastantin, "Technique to counter active echo cancellation of self-protection ISRJ," *Electron. Lett.*, vol. 53, no. 10, pp. 680–681, May 2017. doi: 10.1017/S1759078717000708.
[15] R. Shen, Z. Liu, J. Sui, and X. Wei, "Study on interrupted-sampling repeater jamming performance based on intra-pulse frequency coded signal," *Proc. SPIE*, vol. 10420, Jul. 2017, Art. no. 104204N.
[16] C. Zhou, F. Shi, and Q. Liu, "Research on parameters estimation and suppression for C&I jamming," in *Proc. CIE Int. Conf. Radar*, Oct. 2016, pp. 1–4.
[17] C. Zhou, Q. Liu, and X. Chen, "Parameter estimation and suppression for DRFM-based interrupted sampling repeater jamme," *IET Radar, Sonar Navigat.*, vol. 12, no. 1, pp. 56–63, 2018.
[18] S. Gong, X. Wei, and X. Li, "ECCM scheme against interrupted sampling repeater jammer based on time-frequency analysis," *J. Syst. Eng. Electron.*, vol. 25, no. 6, pp. 996–1003, Dec. 2014. doi: 10.1109/JSEE.2014.00114.
[19] X. Wei, G. Zhang, and W. Liu, "Efficient filter design against interrupted sampling repeater jamming for wideband radar," *EURASIP J. Adv. Signal Process.*, vol. 9, pp. 1–12, Dec. 2017. doi: 10.1186/s13634-017-0446-3.
[20] H. Yuan, C. Wang, X. Li, and L. An, "A method against interrupted-sampling repeater jamming based on energy function detection and band-pass filtering," *Int. J. Antennas Propag.*, vol. 2017, Mar. 2017, Art. no. 6759169. doi: 10.1155/2017/6759169.
[21] J. Chen, W. Wu, S. Xu, Z. Chen, and J. Zou, "Band pass filter design against interrupted-sampling repeater jamming based on time-frequency analysis," *IET Radar, Sonar Navigat.*, to be published.
[22] S. Paul and L. Singh, "A review on advances in deep learning," in *Proc. IEEE Workshop Comput. Intell., Theories, Appl. Future Directions*, Dec. 2015, pp. 1–6.
[23] J. Chen, S. Xu, and Z. Chen, "Convolutional neural network for classifying space target of the same shape by using RCS time series," *IET Radar, Sonar Navigat.*, vol. 12, no. 11, pp. 1268–1275, Nov. 2018.
[24] X. X. Zhu, D. Tuia, L. Mou, G.-S. Xia, L. Zhang, F. Xu, and F. Fraundorfer, "Deep learning in remote sensing: A comprehensive review and list of resources," *IEEE Geosci. Remote Sens. Mag.*, vol. 5, no. 4, pp. 8–36, Dec. 2017.
[25] Z.-Q. Zhao, P. Zheng, S.-T. Xu, and X. Wu, "Object detection with deep learning: A review," *IEEE Trans. Neural Netw. Learn. Syst.*, to be published.
[26] S. Hochreiter and J. Schmidhuber, "Long short-term memory," *Neural Comput.*, vol. 9, no. 8, pp. 1735–1780, 1997.
[27] F. A. Gers, J. Schmidhuber, and F. Cummins, "Learning to forget: Continual prediction with LSTM," *Neural Comput.*, vol. 12, no. 10, pp. 2451–2471, 2000.
[28] J. Chung, C. Gulcehre, K. Cho, and Y. Bengio, "Empirical evaluation of gated recurrent neural networks on sequence modeling," Dec. 2014, *arXiv:1412.3555*. [Online]. Available: https://arxiv.org/abs/1412.3555
[29] K. Cho, B. V. Merrënboer, D. Bahdanau, and Y. Bengio, "On the properties of neural machine translation: Encoder-decoder approaches," in *Proc. 8th Workshop Syntax, Semantics Struct. Stat. Transl.*, Doha, Qatar, Oct. 2014, pp. 103–111.
[30] K. Cui, W. Wu, J. Huang, X. Chen, and N. Yuan, "DOA estimation of LFM signals based on STFT and multiple invariance ESPRIT," *Int. J. Electron. Commun.*, vol. 77, pp. 10–17, Jul. 2017.
[31] B. Tian, Z. Lu, Y. Liu, and X. Li, "Review on interferometric ISAR 3D imaging: Concept, technology and experiment," *Signal Process.*, vol. 153, pp. 164–187, Dec. 2018.
[32] A. L. Maas, A. Y. Hannun, and A. Y. Ng, "Rectifier nonlinearities improve neural network acoustic models," in *Proc. 30th Int. Conf. Mach. Learn.*, Atlanta, GA, USA, 2013, pp. 1–6.
[33] R. A. Dunne and N. A. Campbell, "On the pairing of the softmax activation and cross-entropy penalty functions and the derivation of the softmax activation function," in *Proc. 8th Aust. Conf. Neural Netw.*, 1997, pp. 181–185.
[34] M. D. Zeiler, "ADADELTA: An adaptive learning rate method," Dec. 2012, *arXiv:1212.5701*. [Online]. Available: https://arxiv.org/abs/1212.5701
[35] J. Duchi, E. Hazan, and Y. Singer, "Adaptive subgradient methods for online learning and stochastic optimization," *J. Mach. Learn. Res.*, vol. 12, pp. 2121–2159, Feb. 2011.
[36] W. Jiang, Y. Huang, and J. Yang, "Automatic censoring CFAR detector based on ordered data difference for low-flying helicopter safety," *Sensors*, vol. 16, no. 7, p. 1055, 2016.

JIAN CHEN was born in Hunan, China, in 1991. He received the B.S. degree in electronic science and technology from Tsinghua University, Beijing, China, in 2013, and the M.S. degree in information and communication engineering from the National University of Defense Technology, Changsha, China, in 2015, where he is currently pursuing the Ph.D. degree in information and communication engineering. His research interests include radar signal processing and automatic target recognition.

SHIYOU XU was born in Hebei, China, in 1978. He received the B.S. and Ph.D. degrees from the National University of Defense Technology, Changsha, China, in 2001 and 2008, respectively. From 2008 to 2018, he was a Lecturer with the National University of Defense Technology. He is currently an Associate Professor and a Ph.D. Supervisor with the School of Electronics and Communication Engineering, Sun Yat-sen University, Guangzhou, China. His research interests include radar signal processing and radar target recognition.

JIANGWEI ZOU was born in Ji'an, Jiangxi, China, in 1981. He received the B.S. and M.S. degrees in information engineering from the National University of Defense Technology, Changsha, China, in 2004, and the Ph.D. degree in electronic science and technology, in 2016. He is currently an Assistant Researcher with the ATR Laboratory, National University of Defense Technology. His current research interests include radar signal processing and automatic target recognition.

ZENGPING CHEN was born in Fujian, China, in 1967. He received the B.S. and Ph.D. degrees from the National University of Defense Technology, Changsha, China, in 1987 and 1994, respectively, where he was a Professor and a Ph.D. Supervisor, from 1994 to 2018. He is currently a Professor and a Ph.D. Supervisor with the School of Electronics and Communication Engineering, Sun Yat-sen University. His major research interests include signal processing, radar system, and automatic target recognition.